J. Am. Chem. Soc. 1984, 106, 2621-2625

Host–Guest Molecular Inclusion Type Complex of *N*,*N'*,*N''*,*N'''*-Tetramethyl-2,11,20,29-tetraaza[3.3.3.3]paracyclophane with $CHCl_3$ (Type I Complex) and CH_2Cl_2 (Type II Complex)

Iwao Tabushi,*[†] Kazuo Yamamura,[†] Hiroshi Nonoguchi,[†] Ken Hirotsu,[‡] and Taiichi Higuchi[‡]

Contribution from the Department of Synthetic Chemistry, Kyoto University, Sakyoku, Kyoto, 606 Japan, and the Department of Chemistry, Osaka-City University, Sumiyoshi-ku, Osaka, 558 Japan.

Received July 5, 1983. Revised Manuscript Received December 30, 1983

Abstract: Host–guest (1:1) molecular complexes of *N,N',N'',N'''*-tetramethyl-2,11,20,29-tetraaza[3.3.3.3]paracyclophane (**1**) with $CHCl_3$, CH_2Cl_2, CH_2BrCl, and CH_3CN are reported, and the crystal structures of a $\mathbf{1}\cdot CHCl_3$ complex and a $\mathbf{1}\cdot CH_2Cl_2$ complex have been determined by single-crystal X-ray diffraction methods. The $\mathbf{1}\cdot CHCl_3$ complex belongs to the monoclinic space group $C2$ (chiral) having cell dimensions a = 25.166 (8) Å, b = 5.668 (2) Å, c = 13.438 (4) Å, β = 111.31 (3)°, and Z = 2. The final R value was 0.098 for 1219 reflections measured by Mo Kα radiation. The shape of the heterocyclophane **1** was found to resemble a "square box", with walls formed by benzene rings and the floor being the plane containing the four N atoms. This unique molecular shape results from the conformation of the slightly tilted benzene walls (ca. 60°) with respect to the plane defined by the four N atoms. Thus, **1** provides an appropriately sized cavity (4.6–6.4-Å side width and ca. 6-Å depth), so that **1** includes $CHCl_3$ as a guest molecule with a nearly maximum van der Waals stabilization. In the crystal structures, **1** shows no symmetry element except the C_2 axis and, therefore, **1** is chiral (only in the crystalline state) and exists as optically active isomers, the "*R*" conformer or the "*S*" conformer (type I inclusion crystal). However, when the chiral crystal, $\mathbf{1}\cdot CHCl_3$, was dissolved in chloroform, the resultant solution was optically *inactive*, and the $R \rightleftarrows S$ interconversion rate estimated by ^{1}H NMR was found to be rapid even at −90 °C. $\mathbf{1}\cdot CH_2Cl_2$, on the other hand, crystallizes in a different space group $C2/c$, with the cell dimensions a = 25.359 (5) Å, b = 5.485 (8) Å, c = 50.565 (8) Å, β = 96.92 (3)°, and Z = 8 (R factor = 0.079). This indicates a remarkable contrast between the $\mathbf{1}\cdot CHCl_3$ and the $\mathbf{1}\cdot CH_2Cl_2$ complexes. This is evident from the fact that host **1** of the latter crystal assumed both *R* and *S* conformation, and each conformer made its own packed column (along the *b* axis). "*RR*" columns and "*SS*" columns appear alternatively along the *c* axis (type II complex) in the $\mathbf{1}\cdot CH_2Cl_2$ complex. It is concluded, therefore, that polymorphism of crystallization is induced by inclusion of different guest molecules into the cavity of the host molecule, heterocyclophane **1**. The small stabilization energy thus gained by the change in the host conformation is amplified by making a crystal lattice, leading to the entirely different total crystal structure.

Intense interest in the preparation of completely artificial inclusion hosts[1-4] stems from the need for models of biologically important molecules such as enzymes or receptors. Wide variation is possible in designing host structures that will have the most appropriate size, shape, and functionality for *specific molecular recognition*.[2-4] The cyclodextrin family (α-, β-, γ-, etc.) is one of this class of compounds that has recently been under active investigation.[4] We have been studying the chemistry of higher [2^n]paracyclophanes (n = 4–6, 8) or heterocyclophanes **1–3**, as

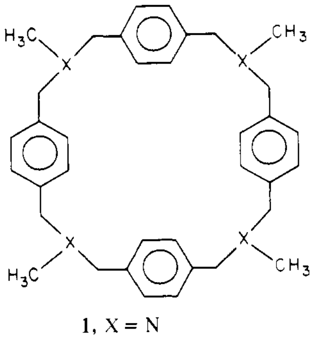

1, X = N
2, X = $NCH_3{}^+BF_4{}^-$
3, X = $S^+BF_4{}^-$

another promising class of completely artificial hosts.[1,2] We have successfully demonstrated that they exhibit enzyme-like or receptor-like functions with remarkable substrate specificity.[1,2]

Scheme I

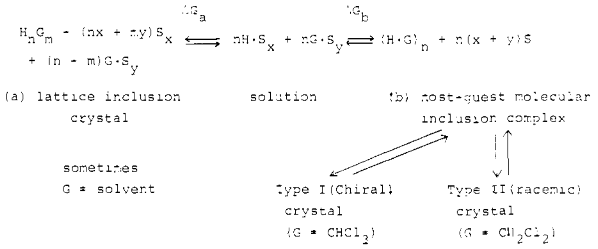

Several different types of cyclophanes have been synthesized by other groups, providing interesting enzyme models.[3]

However, only a limited number of host–guest pairs have had their crystal structures elucidated.[5] Most of these were determined

---

[†] Kyoto University.

[‡] Osaka-City University.

(1) (a) Tabushi, I.; Yamada, H.; Yoshida, Z.; Oda, R. *Tetrahedron* **1971**, *27*, 4845. (b) Tabushi, I.; Yamada, H.; Kuroda, Y. *Ibid.* **1972**, *28*, 3381. (c) Tabushi, I.; Yamada, H.; Yoshida, Z.; Obuchi, K. *Shokubai* **1972**, *14*, 147. (d) Tabushi, I.; Kuroda, Y. *Ibid.* **1974**, *16*, 18.

(2) (a) Tabushi, I.; Sasaki, H.; Kuroda, Y. *J. Am. Chem. Soc.*, **1976**, *98*, 5727. (b) Tabushi, I.; Kuroda, Y.; Kimura, Y. *Tetrahedron Lett.* **1976**, 8827. (c) Tabushi, I.; Kimura, Y.; Yamamura, K. *J. Am. Chem. Soc.* **1978**, *100*, 1304; (d) *Ibid.* **1981**, *103*, 6486.

(3) (a) Murakami, Y.; Aoyama, Y.; Kida, M.; Nakano, A. *Bull. Chem. Soc. Jpn.* **1977**, *50*, 3365. (b) Murakami, Y.; Aoyama, Y.; Kida, M.; Nakano, A.; Dobashi, K.; Tram, C. D.; Matsuda, Y. *J. Chem. Soc., Perkin Trans. 1* **1979**, 9560. (c) Murakami, Y.; Nakano, A.; Miyata, R.; Matsuda, Y. *Ibid.* **1979**, 1669. (d) Reference 5a. (e) Jarvi, E. T.; Whitlock, H. W., Jr. *J. Am. Chem. Soc.* **1980**, *102*, 657. (f) Adams, S. P.; Whitlock, H. W. *Ibid.* **1982**, *104*, 1602.

(4) For a review, see: Tabushi, I. *Acc. Chem. Res.* **1982**, *15*, 66.

0002-7863/84/1506-2621$01.50/0

Table I. Molar Ratio of Guest to Heterocyclophane I in Inclusion Complex

inclusion complex	[guest]/1	
	^{1}H NMR	GLPC
$\mathbf{1}\cdot CHCl_3$		0.90 ± 0.01[b]
$\mathbf{1}\cdot CH_2Cl_2$	0.91 ± 0.02[a]	0.88 ± 0.06[b]
$\mathbf{1}\cdot CH_2BrCl$	1.07 ± 0.07[a]	0.97 ± 0.03[b]
$\mathbf{1}\cdot CH_3CN$	0.90, 0.89	

[a] Mean value of eight measurements. [b] Mean value of four measurements.

Table II. Crystal Data of Inclusion Complexes of *N,N′,N″,N‴*-Tetramethyl-2,11,20,29-tetraaza[3.3.3.3]-paracyclophane (**1**)

	space group	cell constants
$CHCl_3$	*C*2 (chiral)	$a = 25.166$ (8) Å $b = 5.668$ (2) Å $c = 13.438$ (4) Å $\beta = 111.31$ (3)° $Z = 2$
CH_2Cl_2	*C*2/*c*	$a = 25.359$ (5) Å $b = 5.485$ (8) Å $c = 50.565$ (8) Å $\beta = 96.92$ (3)° $Z = 8$

Table III. Fractional Coordinates for $\mathbf{1}\cdot CHCl_3$[a]

atom	*x*	*y*	*z*
C(1)	0.3256 (4)	0.035 (3)	−0.1135 (7)
C(2)	0.3029 (4)	−0.119 (3)	−0.0566 (8)
C(3)	0.3107 (4)	−0.055 (3)	0.0507 (7)
C(4)	0.3379 (4)	0.146 (3)	0.0971 (7)
C(5)	0.3592 (5)	0.293 (3)	0.0387 (8)
C(6)	0.3528 (5)	0.241 (3)	−0.0654 (8)
C(7)	0.3444 (4)	0.221 (3)	0.2093 (8)
C(8)	0.4377 (4)	0.032 (2)	0.299 (1)
C(9)	0.5020 (4)	0.065 (2)	0.3330 (7)
C(10)	0.5363 (4)	−0.120 (2)	0.3878 (7)
C(11)	0.5953 (4)	−0.089 (3)	0.4089 (8)
C(12)	0.6196 (4)	0.092 (2)	0.3755 (7)
C(13)	0.5814 (4)	0.272 (3)	0.3190 (8)
C(14)	0.5230 (5)	0.261 (3)	0.2995 (9)
C(15)	0.6836 (4)	0.113 (3)	0.3971 (6)
C(16)	0.6787 (5)	−0.029 (3)	0.2251 (8)
C(17)	0.4106 (5)	0.370 (3)	0.3793 (8)
C(18)	0.7544 (5)	0.228 (5)	0.329 (1)
N(1)	0.4051 (3)	0.251 (2)	0.2778 (5)
N(2)	0.6935 (3)	0.169 (2)	0.2977 (6)
Cl(1)	0.491 (1)	−0.134 (5)	0.093 (2)
Cl(2)	0.481 (1)	−0.208 (5)	−0.123 (1)
Cl(3)	0.5174 (9)	−0.589 (4)	0.028 (2)
C(19)	0.5193 (7)	−0.283 (5)	0.010 (1)

[a] Standard deviations of the least significant figures are given in parentheses.

to belong to the "lattice inclusion crystal" type of host–guest complex H_nG_m (case a, Scheme I), where significant host–host interaction affords a cage or a channel between host molecules for guest accommodation.[6] This leads to relatively poor guest selectivity. The ratio n/m varies significantly, e.g., from 0.3–0.6 for cyclotricatechylene (**4**)[5b] to 2–6 for tri-*o*-thymotide (**5**).[7] Optical resolution of 2-butyl halide by **5**[7a] is thus attributed to the crystal lattice chirality that was induced by the H_2G_1 crystallization. In only a few cases, a molecular (one to one) inclusion crystal, $(H\cdot G)_n$ (case b, Scheme I) was reported.[5a,8]

Here the authors wish to report that a host–guest (1:1) molecular inclusion crystal $(H\cdot G)_n$ (Scheme I) has been obtained from **1**[9] and $CHCl_3$ or CH_2Cl_2. Evidence of this was provided through the use of X-ray crystal structure analysis. Furthermore, GLPC determination and spectroscopic measurements (NMR, IR) demonstrated the formation of other 1:1 complexes of $\mathbf{1}\cdot G$ ($G = CH_2BrCl$, CH_3CN). It was found that host **1**, with an approximately square conformation (Figure 1), formed a stable complex with $G_I = CHCl_3$ with nearly maximum van der Waals (vdW) stabilization. This results in either all-*R* inclusion crystallization $(R\text{-}\mathbf{1}\cdot G_I)_n$ or all-*S* inclusion crystallization $(S\text{-}\mathbf{1}\cdot G_I)_n$ ($G_I = CHCl_3$) (type I chiral crystal, eq 1). In contrast, it is interesting to note that a racemic inclusion crystal $[(R\text{-}\mathbf{1}\cdot G_{II})_2(S\text{-}\mathbf{1}\cdot G_{II})_2]_n$ forms when G_{II} is CH_2Cl_2 (eq 2, type II racemic crystal). The host–guest stabilization of the latter was optimized by **1** through a slight decrease in the cavity size (especially in the *c*-axis direction) and slightly increased tilt of the benzene walls. Thus, the selection of crystal type, type I (chiral) or type II (racemic), is mainly determined by the *host–guest pairwise* interaction. A small difference in the host–guest interaction energy in a host–guest pair results in a difference in the host conformation. The small energy difference is "amplified" or "accumulated" to determine the total intercolumn interaction, giving type I crystal (*RR* conformation) or type II crystal (*RS* conformation) depending on the size and shape of a guest.

$$R\text{-}\mathbf{1}\cdot G_{(I\ \mathrm{or}\ II)} \rightleftarrows S\text{-}\mathbf{1}\cdot G \xrightarrow{\text{type I}} \underset{\substack{\text{chiral complex} \\ G_I = CHCl_3}}{(R\text{-}\mathbf{1}\cdot G_I)_n \text{ or } (S\text{-}\mathbf{1}\cdot G_I)_n} \tag{1}$$

$$R\text{-}\mathbf{1}\cdot G_{(I\ \mathrm{or}\ II)} \rightleftarrows S\text{-}\mathbf{1}\cdot G \xrightarrow{\text{type II}} \underset{\substack{\text{racemic complex } (RRSS) \\ G_{II} = CH_2Cl_2}}{[(R\text{-}\mathbf{1}\cdot G_{II})_2(S\text{-}\mathbf{1}\cdot G_{II})_2]_n} \tag{2}$$

Results and Discussion

Molecular Inclusion Crystal of $\mathbf{1}\cdot CHCl_3$. A host–guest inclusion-type crystal was obtained from heterocyclophane **1** and $CHCl_3$. The properties of this crystal were investigated spectroscopically (NMR, IR) and by X-ray diffraction methods (see next paragraph).

The IR spectrum of the $\mathbf{1}\cdot CHCl_3$ crystal showed a new strong absorption at ~760 cm^{-1} in addition to the characteristic absorptions of **1**. This band has previously been assigned as a C–Cl stretch. The complex was unchanged after 6 h of heating at 50 °C (0.4 mmHg), on the basis of the fact that the IR intensity remained constant to within 1%. However, the crystal was destroyed with the concomitant total loss of $CHCl_3$ upon 4 h of heating at 80 °C (0.5 mmHg). A selective crystallization of $\mathbf{1}\cdot CHCl_3$ was also achieved by using an appropriate solvent such as *n*-hexane, which is a poor guest. Chloroform in the crystal was determined by GLPC (t_R = 37 min at 50 °C on DC 550, 6 m with 0.8 kg/cm^2 He) and the observed $CHCl_3/\mathbf{1}$ ratio was 0.90 ± 0.01 (Table I).

Molecular Structure of $\mathbf{1}\cdot CHCl_3$ Complex. X-ray analysis was carried out on a $\mathbf{1}\cdot CHCl_3$ single crystal (see Experimental Section). Unit cell parameters determined at 25 °C are given in Table II. The full-matrix least-squares refinement, with $CHCl_3$ (guest

---

(5) (a) Odashima, K.; Itai, A.; Iitaka, Y.; Koga, K. *J. Am. Chem. Soc.* **1980**, *102*, 2504. (b) Hyatt, J. A.; Duesler, E. N.; Curtin, D. Y.; Paul, I. C. *J. Org. Chem.* **1980**, *45*, 5074. (c) Ichikawa, Y.; Tsuruta, H.; Kato, K.; Yamamaka, Y.; Yamamoto, M. *Japan Kokai* **1977**, 51329; *Chem. Abstr.* **1977**, *87*, 134101*p*; *Ibid* **1978**, *78*, 65859; *Chem. Abstr.* **1978**, *89*, 1971375. Yamaji, T.; Yoshisato, E.; Hiramatsu, T. *Ibid.* **1978**, *78*, 21151; *Chem. Abstr.* **1978**, *89*, 42589*s*; *Ibid.* **1978**, *78*, 21144; *Chem. Abstr.* **1978**, *89*, 6017*v*; *Ibid.* **1978**, *87*, 21150; *Chem.* Abstr. **1978**, *89*, 42730*f*. (d) Inclusion complex claimed, but no X-ray study: Stetter, H.; Roos, E. E. *Ber.* **1955**, *88*, 1390. Faust, G.; Pallas, M. *J. Prakt. Chem.* **1960**, *11*, 146. (e) Andreetti, G. D.; Ungaro, R.; Pochinic, A. *J. Chem. Soc., Chem. Commun.* **1979**, 1005.

(6) The presence of hydrogen bonding was demonstrated by X-ray as the host–host interaction in complexes of cyclotricatechylene (**4**).[5b]

(7) (a) Powell, H. M. *Nature (London)* **1952**, 155. (b) Lawton, D.; Powell, H. M. *J. Chem. Soc.* **1958**, 2339. (c) Downing, A. P.; Ollis, W. D.; Sutherland, I. O. *J. Chem. Soc., Chem. Commun.* **1968**, 329. (d) Williams, D. J.; Lawton, D. *Tetrahedron Lett.* **1975**, 111. (e) Williams, D. J. *J. Chem. Soc., Chem. Commun.* **1977**, 170. (f) Gerdil, R.; Allemand, J. *Helv. Chim. Acta* **1980**, *63*, 1750. (g) A-Yellin, R.; Green, B. S.; Knossow, M.; Tsoucaris, G. *Tetrahedron Lett.* **1980**, 387. (h) Unal, G. G.; Williams, D. J. *Ibid.* **1981**, *22*, 2225..

(8) Abbott, S. J.; Barrett, A. G. M.; Godfrey, C. R. A.; Kalindjian, S. B.; Simpson, G. W.; Williams, D. J. *J. Chem. Soc., Chem. Commun.* **1982**, 796.

(9) The first prepartion of **1** appeared in: Urushigawa, Y.; Inazu, T.; Yoshino, T. *Bull. Chem. Soc. Jpn.* **1971**, *44*, 2546. And was modified by us in ref 2b.

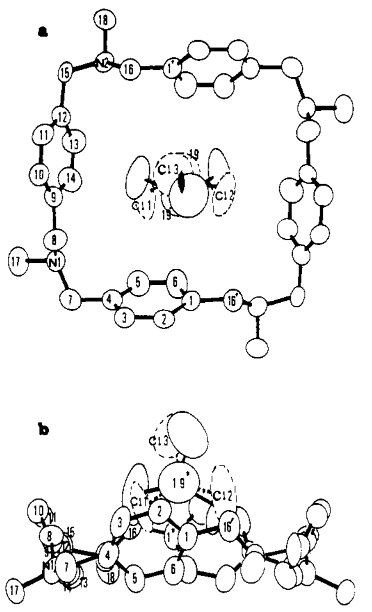

Figure 1. Perspective view of 1·$CHCl_3$ chiral inclusion complex determined by the X-ray method.

molecule) as a rigid body, converged to $R = 0.098$, and the fractional atomic coordinates are listed in Table III (and in Table IV for the CH_2Cl_2 complex). Selected conformational angles and nonbonded distances are given in Table V.

The macrocyclic shape (shown in Figure 1a) of **1** is highly dependent on the local conformation of the four CH_2–N(CH_3)–CH_2 segments. The dihedral angle has been determined as C(7)–N(1)–C(8)–C(9) or C(15)–N(2)–C(16)–C(1′), 159–166°, and C(4)–C(7)–N(1)–C(8) or C(12)–C(15)–N(2)–C(16), 66–69°, respectively. Therefore, the gauche-trans conformation[10] in the CH_2–N(CH_3)–CH_2 segments constitutes the characteristic feature of the macrocycle **1**.

As a result of this conformation, **1** takes on a unique molecular shape resembling a "square box" (Figure 1). The walls are composed of four benzene rings that form angles of ca 60° with respect to a pseudo molecular plane defined by the four N atoms. This conformation is achieved by rotation of the benzene rings around the C(7)–C(4)–C(1)–C(16′) or C(15)–C(12)–C(9)–C(8) axis.

Noteworthy is that a $CHCl_3$ molecule is included in the cavity of **1**—*molecular inclusion*—as shown in Figure 1, in sharp contrast to abundant examples of "lattice inclusion" complexes such as those of tri-*o*-thymotide and cyclotricatechylene. The Cl–host distance has been determined as Cl(1)- - -C(8) = 3.61, Cl(1)- - -C(9) = 3.33, Cl(1)- - -C(14) = 3.42, Cl(2)- - -C(9′) = 3.38, Cl(2)- - -C(14′) = 3.54, Cl(2)- - -C(10′) = 3.46 Å, respectively, being very close to the sum of van der Waals radius (r_{vdW}) 1.80 Å of Cl + 1.70 Å of C^{sp^2} = 3.5 Å. Therefore, $CHCl_3$ is included by **1** completely inside the cavity with nearly maximum van der Waals stabilization.[11]

Several vdW contacts were also seen between Cl(3), which is not in the cavity of **1**, and the next host molecule; Cl(3)- - -C′(6) = 3.28, Cl(3)- - -C′(5) = 3.59 Å. From preliminary reports, similar contacts are also seen for a complex involving **1** and a larger guest, dioxane.[8] Packing of 1·$CHCl_3$ pairs in the crystal is shown in Figure 2a. It can be seen that the vertical (molecular stack) is parallel to the *b* axis (identical with the C_2 axis direction). Thus, host **1** with "*R*" conformation makes "*R*" columns, which are further packed in both *a* and *c* directions (Figure 2).

Table IV. Fractional Coordinates for 1·CH_2Cl_2[a]

atom	*x*	*y*	*z*
C(1)	0.7292 (2)	0.437 (1)	0.1550 (1)
C(2)	0.6932 (2)	0.601 (1)	0.1428 (1)
C(3)	0.6712 (2)	0.573 (1)	0.1165 (1)
C(4)	0.6855 (2)	0.383 (1)	0.1017 (1)
C(5)	0.7216 (2)	0.217 (1)	0.1135 (1)
C(6)	0.7428 (2)	0.243 (1)	0.1401 (1)
C(7)	0.6625 (2)	0.346 (1)	0.0728 (1)
C(8)	0.7329 (2)	0.556 (1)	0.0532 (1)
C(9)	0.7876 (2)	0.518 (1)	0.0451 (1)
C(10)	0.8101 (2)	0.692 (1)	0.0301 (1)
C(11)	0.8625 (2)	0.669 (1)	0.0248 (1)
C(12)	0.8930 (2)	0.472 (1)	0.0338 (1)
C(13)	0.8690 (2)	0.298 (1)	0.0481 (1)
C(14)	0.8184 (2)	0.322 (1)	0.0537 (1)
C(15)	0.9493 (2)	0.443 (2)	0.0278 (1)
C(16)	0.9914 (2)	0.559 (1)	0.0715 (1)
C(17)	1.0154 (2)	0.467 (1)	0.0982 (1)
C(18)	1.0549 (2)	0.590 (1)	0.1137 (1)
C(19)	1.0745 (2)	0.511 (1)	0.1390 (1)
C'(20)	1.0547 (2)	0.306 (1)	0.1497 (1)
C(21)	1.0151 (2)	0.175 (1)	0.1343 (1)
C(22)	0.9960 (2)	0.257 (1)	0.1088 (1)
C(23)	1.0761 (2)	0.206 (1)	0.1766 (1)
C(24)	1.0073 (2)	0.381 (1)	0.2003 (1)
C(25)	0.9527 (2)	0.338 (1)	0.2081 (1)
C(26)	0.9304 (2)	0.506 (1)	0.2234 (2)
C(27)	0.8783 (2)	0.486 (1)	0.2290 (1)
C(28)	0.8473 (2)	0.290 (1)	0.2190 (1)
C(29)	0.8700 (2)	0.117 (1)	0.2044 (1)
C(30)	0.9218 (2)	0.143 (1)	0.1990 (1)
C(31)	0.7897 (2)	0.267 (1)	0.2242 (1)
C(32)	0.7547 (2)	0.472 (1)	0.1833 (1)
C(33)	0.6814 (3)	0.251 (1)	0.0287 (1)
C(34)	1.0360 (3)	0.288 (2)	0.0442 (1)
C(35)	1.0556 (2)	0.030 (1)	0.2179 (1)
C(36)	0.7001 (2)	0.196 (2)	0.2050 (1)
N(1)	0.7038 (2)	0.328 (1)	0.0549 (1)
N(2)	0.9849 (2)	0.366 (1)	0.0514 (1)
N(3)	1.0343 (2)	0.1576 (9)	0.1937 (1)
N(4)	0.7535 (2)	0.250 (1)	0.1993 (1)
C(37)	0.8571 (5)	0.604 (2)	0.1201 (2)
Cl(1)	0.8864 (1)	0.5706 (8)	0.1501 (1)
Cl(2)	0.8589 (1)	0.8732 (7)	0.1052 (1)

[a] Standard deviations of the least significant figures are given in parentheses.

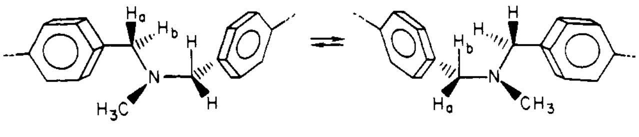

1,*R* conformer 1,*S* conformer

(3)

Molecular Structure of 1·CH_2Cl_2 Inclusion Crystal (Type II Crystal). An interesting discovery occurred when the crystal structure of 1·CH_2Cl_2 was studied by the X-ray diffraction. 1·CH_2Cl_2 forms *racemic* inclusion crystals, of which crystal data are given in Table II. A schematic pattern of the 1·CH_2Cl_2 packing (Figure 2b) shows two *R* and two *S* columns appearing alternately along the *c*-axis direction—i.e., the molecular inclusion crystal of 1·CH_2Cl_2 has the formula of $[(R\text{-}\mathbf{1}\cdot G_{II})_2(S\text{-}\mathbf{1}\cdot G_{II})_2]_n$ where G_{II} is CH_2Cl_2 (type II).

The *RS* intercolumn contact in the type II crystal is characterized by the presence of a symmetry center, with *S*-**1** host having the inverted orientation of the adjacent *R*-**1** host. By contrast, the *RR* or *SS* contact, related by the C_2 axis (Figure 2b), closely resembles the all-*R* or all-*S* packing of the type I crystal, 1·$CHCl_3$. Therefore, this novel polymorphism of packing in the inclusion crystal is the result of small conformation changes of the host

---

(10) Newman, M. S. "Steric Effects in Organic Chemistry"; Wiley: New York, 1956.

(11) r_{CH} = 1.1$_2$ and r_{vdw}(H) = 1.2 Å: Pauling, L. "Nature of the Chemical Bond"; Cornell University Press: Ithaca, NY, 1960; pp 260, 263.

(12) For the tentative *R* and *S* assignment, we followed the proposal: Cahn, R. S.; Ingold, C.; Prelog, V. *Angew. Chem.* **1966**, *78*, 413. See also: Krow, G. *Top. Stereochem.* **1970**, *5*, 31.

(13) Achiral molecules occassionally crystallize in chiral fashion as one of the referees pointed out. See also: Shudt, E.; Weitz, G. In "Crystal and Solid State Physics"; Hellwege, K.-H., Ed.; Springer-Verlag: Berlin, Vol. 5, 1971; "Structure Data of Organic Crystals".

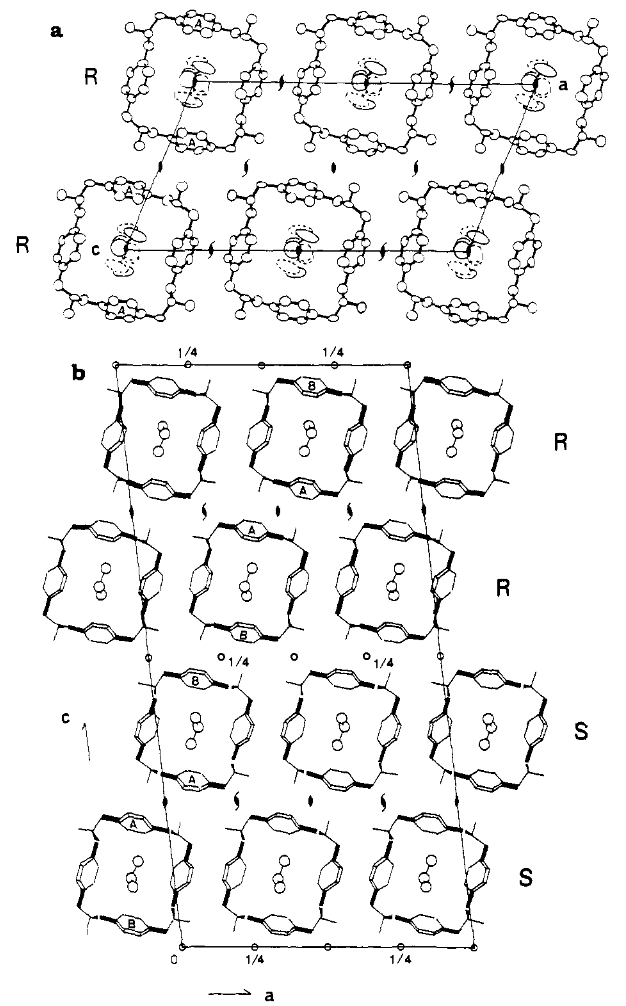

Figure 2. (a) Crystal packing of optical active conformer of **1** in **1**·CHCl$_3$ inclusion complex (viewed along the *b* axis). (b) Crystal packing of *R* and *S* conformers of **1** in **1**·CH$_2$Cl$_2$ inclusion complex (viewed along the *b* axis).

molecule induced by changes in the guest's structure.

Guest-Dependent Polymorphism and Plane Chirality in the Crystalline Host–Guest Packing. Repeated measurements of the optical rotation of the solution of **1**·CHCl$_3$ single crystal dissolved in chloroform indicated, however, that $[\alpha]_D$ of **1** is zero, within the accuracy of the polarimeter, $[\alpha]_D = 0.000 \pm 0.005$ (*c* 0.01). This fact strongly indicates that **1** no longer exhibits chirality in solution.[14] The observations demonstrate that the $R \rightleftarrows S$ conformer change is very rapid in the solution phase. It may have a close connection with the axial–equatorial change of methylene hydrogen(s) observed for [2^4]paracyclophane (**7**) by ^{1}H NMR.[1b,15]

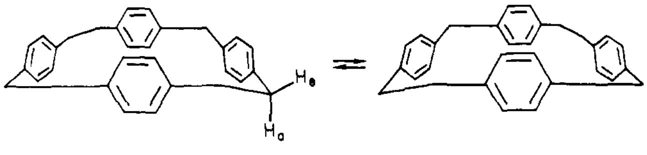

[2^4]paracyclophane (7)

Temperature-dependent ^{1}H NMR measurements of **1** in CS$_2$ showed no line splitting. Moderate line broadening alone, was observed as the temperature was lowered to −95 °C. At that temperature, the ratio of the full width at half of the maximum peak height ($\delta_{\nu_{1/2}}$) of the methylene protons of **1** (δ 3.33) to $\delta_{\nu_{1/2}}$ of CH$_2$Cl$_2$ (standard) was 6.2 and $\delta_{\nu_{1/2}}^{\text{arom}}/\delta_{\nu_{1/2}}^{\text{CH}_2\text{Cl}_2} = 30$, $\delta_{\nu_{1/2}}^{\text{CH}_3}/\delta_{\nu_{1/2}}^{\text{CH}_2\text{Cl}_2} = 9.0$. Therefore, it was concluded that the conformation changes are rapid, even at −95 °C, and still faster at room temperature.

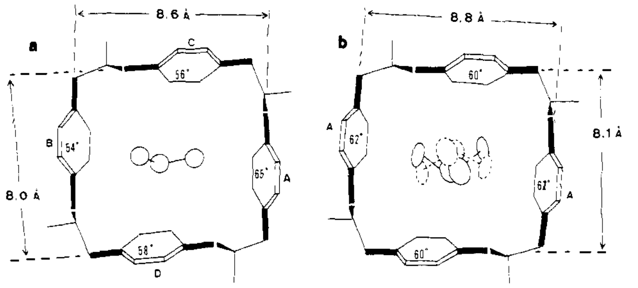

Figure 3. Schematic comparison of macroring conformation of **1** between (a) **1**·CH$_2$Cl$_2$ molecular inclusion and (b) **1**·CHCl$_3$ molecular inclusion.

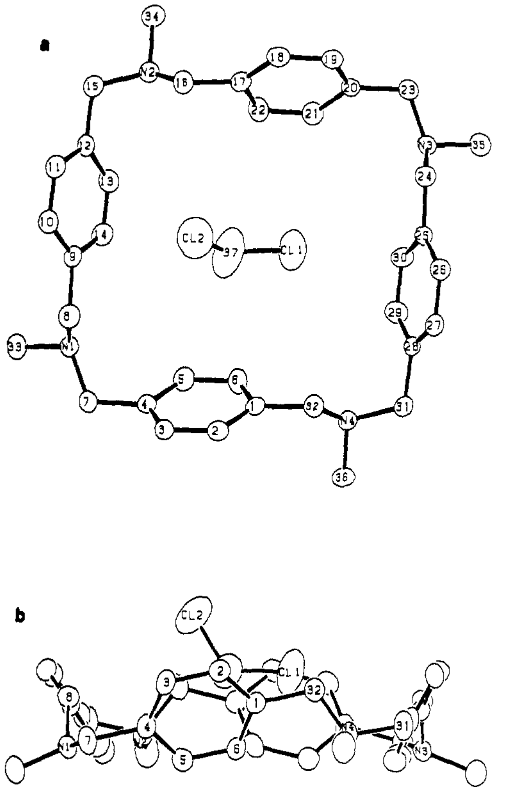

Figure 4. Perspective view of **1**·CH$_2$Cl$_2$ inclusion complex determined by the X-ray method.

In the crystalline phase, however, the conformation is frozen, due to the lattice energy operating between host molecules. Thus the conformation is fixed, either all *R* or all *S* state. The probability of an all *R* or an all *S* crystal must be 50% and 50%, respectively.

Either the all *R* or all *S* conformer are well-ordered in the chiral inclusion crystal **1**·CHCl$_3$ (type I) as shown in Figure 2a, and the intercolumn geometry in the *c*-axis direction, *R–R* column contact, is related by a 180° rotation around the C_2 axis. Thus, "wall to wall" contact is made between two adjacent host molecules, and the crystal is made by packing the layer of *R* column in this *c*-axis direction.

Figure 3 shows a schematic comparison between the host structure in **1**·CHCl$_3$ (type I) and in **1**·CH$_2$Cl$_2$ (type II). The length of one side of the type I host was determined to be 8.8 Å, considerably longer than the other side, 8.1 Å (Figure 3a). This measurement was made using the distance between the two straight lines connecting C(9) and C(12) of the benzene plane. The dimension of type I host along the *c*-axis direction is slightly longer than the length of the corresponding side, 8.6 Å, of a type II host (Figure 3b). This strongly indicates that the type I host

---

(14) Attempted measurement indicated that the optical rotation $[\alpha]_D$ of **1** is less than the accuracy of polarimeter 0.001 (*c* 0.01).

(15) *Evaluation of intermolecular rate process by dynamic NMR* is discussed in details by G. Binsch, especially on the scattered E_a value depending on the approximation. Binsch, G. *Top. Stereochem.* **1968**, *3*, 97–192.

Table V. Selected Conformational Angles (deg) and Host–Guest Nonbonded Distances (Å) of $1\cdot CHCl_3$ and $1\cdot CH_2Cl_2$

	$1\cdot CHCl_3$		
C(3)–C(4)–C(7)–N(1)	122 (1)	Cl(1)···C(8)	3.61 (3)
C(5)–C(4)–C(7)–N(1)	−60 (2)	Cl(1)···C(9)	3.33 (3)
C(4)–C(7)–N(1)–C(8)	−66 (1)	Cl(1)···C(10)	3.70 (3)
C(7)–N(1)–C(8)–C(9)	159 (1)	Cl(1)···C(14)	3.42 (3)
N(1)–C(18)–C(9)–C(10)	159 (1)	Cl(2)···C(9′)	3.37 (3)
N(1)–C(8)–C(9)–C(14)	−28 (1)	Cl(2)···C(10′)	3.46 (2)
C(11)–C(12)–C(15)–N(2)	131 (1)	Cl(2)···C(11′)	3.68 (2)
C(13)–C(12)–C(15)–N(2)	−50 (2)	Cl(2)···C(13′)	3.72 (3)
C(12)–C(15)–N(2)–C(16)	−69 (1)	Cl(2)···C(14′)	3.54 (3)
C(15)–N(2)–C(16)–C(1′)	166 (1)		
N(2)–C(16)–C(1′)–C(2′)	138 (1)		
N(2)–C(16)–C(1′)–C(6)	−44 (2)		
	$1\cdot CH_2Cl_2$		
C(3)–C(4)–C(7)–N(1)	125 (1)	C(19)–C(20)–C(23)–N(3)	130 (1)
C(5)–C(4)–C(7)–N(1)	−56 (1)	C(21)–C(20)–C(23)–N(3)	−54 (1)
C(4)–C(7)–N(1)–C(18)	−67 (1)	C(20)–C(23)–N(3)–C(24)	−64 (1)
C(7)–N(1)–C(8)–C(9)	156 (1)	C(23)–N(3)–C(24)–C(25)	158 (1)
N(1)–C(8)–C(9)–C(10)	148 (1)	N(3)–C(24)–C(25)–C(26)	157 (1)
N(1)–C(18)–C(9)–C(14)	−37 (1)	N(3)–C(24)–C(25)–C(30)	−28 (1)
C(11)–C(12)–C(15)–N(2)	136 (1)	C(27)–C(28)–C(31)–N(4)	123 (1)
C(13)–C(12)–C(15)–N(2)	−46 (1)	C(29)–C(28)–C(31)–N(4)	−57 (1)
C(12)–C(15)–N(2)–C(16)	−68 (1)	C(28)–C(31)–N(4)–C(32)	−64 (1)
C(15)–N(2)–C(16)–C(17)	165 (1)	C(31)–N(4)–C(32)–C(1)	165 (1)
N(2)–C(16)–C(17)–C(18)	136 (1)	N(4)–C(32)–C(1)–C(2)	133 (1)
N(2)–C(16)–C(17)–C(22)	−48 (1)	N(4)–C(32)–C(1)–C(6)	−49 (1)
C(37)···C(6)	3.75 (1)	Cl(1)···C(26)	3.757 (7)
C(37)···C(14)	3.72 (1)	Cl(1)···C(29)	3.768 (7)
Cl(1)···C(25)	3.445 (7)	Cl(1)···C(30)	3.449 (8)

has a somewhat more rectangular shape when compared with the type II host. Furthermore, the tilting angles of three benzene planes of the type II host, B, C, and D (Figure 3b), ranging from 32° to 36° are somewhat larger than A in order to achieve the maximum vdW contact with CH_2Cl_2, a relatively small guest molecule (Figure 4).

In conclusion, the guest-dependent polymorphism of packing and plane chirality are of considerable theoretical interest from the viewpoint that small differences in the host–guest interaction may be very critical to the mode of crystal growing process. Although the energy for the interaction is very small, it was most probably "amplified" or "accumulated" to a magnitude large enough to alter the intercolumn interaction, presenting a new aspect of the host–guest chemistry field.

Experimental Section

Materials. *N,N′,N″,N‴*-Tetramethyl-2,11,20,29-tetraaza[3.3.3.3]-paracyclophane (**1**) was prepared as described in our previous paper[2c] (by a modified synthetic procedure of the reported preparation[9]). Preparation of inclusion crystals for the crystallographic studies was carried out by using **1** after purification. Chloroform, *n*-hexane, acetonitrile, methylene chloride, 2-methylbutanol, and bromochloromethane of reagent grade were used without further purification. Carbon disulfide of pure reagent grade was used as a solvent for the low-temperature ^1H NMR experiments.

Physical and Analytical Measurements. Infrared spectra were obtained in KBr pellets by using a Hitachi 215 spectrometer. Low-temperature ^1H NMR experiments and quantitative determination of the amount of included guests were carried out with a Varian HA-100D spectrometer. ^1H NMR measurement for the structure determination was performed with a NEVA PMX-60 spectrometer or a Varian EM 360 spectrometer. Elemental analyses were performed by Microanalysis Laboratory of Kyoto University.

GLPC analyses of guest compounds that were included by **1** were carried out by using a Shimadzu GC 4B-IT gas chromatograph on a Silicon DC-550 column (3 mm $\phi \times 6$ m, 50 °C, He carrier 0.8 kg/cm^2). The retention times of $CHCl_3$, CH_2Cl_2, and CH_2BrCl were 37, 21, and 41 min, respectively. Quantitative determination of the amount of the included guest was also made by GLPC. Thus, a small crystal of $\mathbf{1}\cdot CHCl_3$, $\mathbf{1}\cdot CH_2Cl_2$, or $\mathbf{1}\cdot CH_2BrCl$ inclusion complex of a certain weight (4.7–6.3 mg) was dissolved in 0.4–1.0 mL of dioxane, to which was added a 1-mL solution of 1,2-dichloroethane (as an internal standard, $t_R = 54$ min) and analyzed. Quantitative determination was made on the basis of a calibration curve, mole ratio of guest/standard vs. ratio of GLPC peak area, and the results are summarized in Table I.

Crystallization and X-ray Studies. Inclusion crystals of **1** were obtained by slow evaporation of solvent ($CHCl_3$, CH_2Cl_2, CH_2BrCl, or CH_3CN) from a solution of ca. 0.2 g of **1** in 3–50 mL of the solvent in a vial of appropriate volume. The solution in the vial was placed in a dessicator over KOH pellets at room temperature for 1–5 days. For the $CHCl_3$ solvent KOH was not used. The single crystal of $\mathbf{1}\cdot CHCl_3$ thus obtained was transferred into a thin-walled glass capillary and three-dimensional diffraction data consisting of 1750 reflections were collected by $\omega/2\theta$ scan with Mo Kα radiation up to $2\theta = 50°$, 1219 data [$I > 3\sigma(I)$] of which were used for the least-squares refinement. The crystal structure was solved by the direct method. A preliminary crystallographic refinement suggests a disordering of $CHCl_3$ (guest molecule), which was successfully resolved, after the final least-squares refinement, into two $CHCl_3$ molecules related by a 2-fold axis with the refined occupancy factor of 0.42 for each $CHCl_3$ position. Full-matrix least-squares refinement with $CHCl_3$ as a rigid body converged to a conventional discrepancy index of 0.098. For $\mathbf{1}\cdot CH_2Cl_2$ single crystal, three-dimensional diffraction data consisting of 4904 reflections were collected by $\omega/2\theta$ scan with Mo Kα radiation up to $2\theta = 46°$, 2597 data [$I > 3\sigma(I)$] of which were used for the least-squares refinements. The crystal structure was solved by the direct method. Full-matrix least-squares refinement with anisotropic temperature factors have converged to an *R* value of 0.079. The crystal data are summarized in Table II. For the analyses, the following library programs were employed: MULTAN,[16] ORFLS,[17] ORTEP.[18]

Low-temperature ^1H NMR experiments were carried out with Varian HA-100 spectrometer equipped with a variable-temperature accessary V-4341/V-6057 using cooled N_2 gas as the coolant. Temperature calibration was carried out on the basis of the chemical shift change of the MeOH hydroxyl proton.

Registry No. $\mathbf{1}\cdot CHCl_3$, 89321-18-6; $\mathbf{1}\cdot CH_2Cl_2$, 89302-75-0; $\mathbf{1}\cdot CH_2BrCl$, 89302-76-1; $\mathbf{1}\cdot CH_3CN$, 89302-77-2.

Supplementary Material Available: Tables of thermal parameters, bond distances and angles, and structure factors for $\mathbf{1}\cdot CHCl_3$ and $\mathbf{1}\cdot CH_2Cl_2$ inclusion complexes (16 pages). Ordering information is given on any current masthead page.

---

(16) Germain, G.; Main, P.; Woolfson, M. M. *Acta Crystallogr., Sect. B* **1970**, *B26*, 274. And references cited in: Woolfson, M. M. *Acta Crystallogr., Sect. A* **1977**, *A33*, 219.

(17) Busing, W. R.; Martin, K. O.; Levy, H. A. Oak Ridge National Laboratory Report ORNL-TM-305.

(18) Johnson, C. K. Oak Ridge National Laboratory Report ORNL-TM-3794.